Estimating the Hardenability of Carbon Steels

R. A. GRANGE

A new hardenability test for shallow-hardening steels was developed which allows the precise measurement of the hardenability of "pure" Fe-C alloys. The quantitative hardenability effect of variation in the austenite grain size of carbon steels was found to vary linearly with $d_\gamma^{-1/2}$, where d_γ is the mean austenite grain diameter. Using high-purity steels, the quantitative hardenability effects of C and the common alloying elements Mn, P, S, Si, Cu, Ni, Cr, Mo, V, Ti, and Zr were determined. From these data, the hardenability of carbon steels, with and without residual elements, can be estimated from chemical composition and grain size by a new and relatively simple method.

SEVERAL considerations suggest the desirability of returning to basic principles in order to understand and estimate reliably the hardenability of steel from its chemical composition and austenite grain size. Current methods of estimating hardenability are not an unqualified success over broad ranges in chemical composition and grain size.[1] The quantitative hardenability effect of each element, as documented in the literature,[2] varies substantially. The quantitative hardenability effect of variation in austenite grain size has not received adequate attention. Interaction effects among alloying elements are not fully understood. Most hardenability investigations have dealt with medium-carbon steels, although in recent years shallow-hardening, low-carbon steels, which can be water-quenched with little likelihood of cracking, have often replaced medium-carbon, oil-hardening steels; it is unlikely that quantitative hardenability effects of chemical elements and grain size are exactly the same in low- and medium-carbon steels. For economy, carbon steels with hardenability enhanced by higher manganese or residual elements are increasingly replacing low-alloy steels. Estimation of hardenability in shallow-hardening, low-carbon steels should be more reliable than in the more complex low-alloy steels, but the opposite is usually true, at least relative to the more precise knowledge and control of hardenability required in the former for their efficient use.

These considerations led us to attempt a reassessment of the quantitative hardenability effects of carbon, individual alloying elements, and grain size. The obvious starting point is with "pure" Fe-C alloys since the effect of carbon is basic in understanding and estimating hardenability. Emphasis in this investigation is on low-carbon (~0.2 pct) steels, rather than on the medium-carbon steels which heretofore have been favored for hardenability studies.

THE "HOT-BRINE" HARDENABILITY TEST

Reliable measurement of the hardenability of Fe-C alloys, as well as many low-carbon steels, requires a precise and reproducible test. Commonly used hardenability tests, which utilize depth of hardening in a specimen too large to harden throughout, do not provide the desired high precision and reproducibility. Probably the most satisfactory established test procedure for steels of very low hardenability consists of austenitizing and quenching in water or brine a series of cylinders of different diameter. The diameters must vary so that the smallest specimen is through-hardened and the largest unhardened at the center. After quenching, center hardness of the three or more cylinders required is measured. These hardness values are then plotted against cylinder diameter to define a curve from which hardenability may be read off as a "critical" diameter. The method may also use percentage martensite in lieu of hardness. Obviously, this test procedure is tedious and hence unsuitable for routine testing. Therefore, a more convenient hardenability test, hereafter designated the "Hot-Brine" (HB) test, was developed.

Hardenability tests traditionally employ a specimen in which cooling rate decreases with distance from a quenched surface. It is also possible to vary cooling rate in small specimens of fixed dimensions by varying severity of quench. This can be done either by using a variety of quenching media or, more conveniently, by varying the quenching severity of a single medium. It is well known that the quenching severity of water decreases progressively above about 100°F (38°C), and water becomes a very mild quenchant when heated to its boiling point. In preliminary tests, small sheet specimens were austenitized alike and quenched in hot water. As anticipated, the specimens decreased in hardness as the water was hotter, but several specimens quenched alike failed to develop the same hardness. To overcome this erratic behavior, we adopted a brine solution made by adding 6 pct by weight of NaCl to water. This hot brine proved to be a satisfactorily consistent quenchant, especially at temperatures approaching the boiling point of water.

Even with the improvement resulting from adoption of brine, hardness was not always consistent within the central area of the specimen; that is, there were occasional soft spots. Up to this point, specimens were austenitized in an air-muffle furnace and were scaled going into the quenchant. It seemed likely that hardness variation within the specimen was due to nonuniform removal of scale during quenching. An atmosphere

R. A GRANGE is Staff Scientist, Research Laboratory, U. S Steel Corporation, Monroeville, Pa. 15146. This paper is based on a presentation made at a symposium on "Hardenability" held at the Cleveland Meeting of The Metallurgical Society of AIME, October 17, 1972, under the sponsorship of the IMD Heat Treatment Committee.

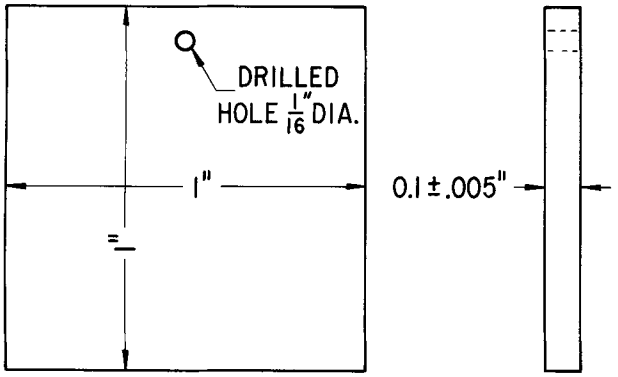

(a) SPECIMEN DIMENSIONS

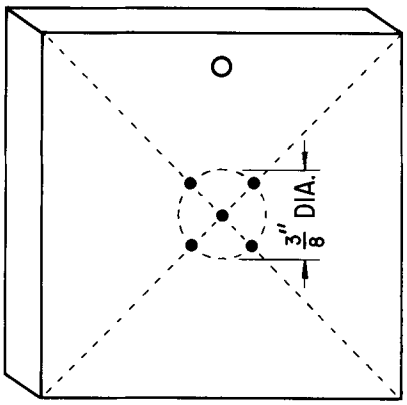

(b) METHOD OF LOCATING Rc HARDNESS IMPRESSIONS AFTER HEAT TREATMENT

Fig. 1—Hot-brine hardenability test specimen.

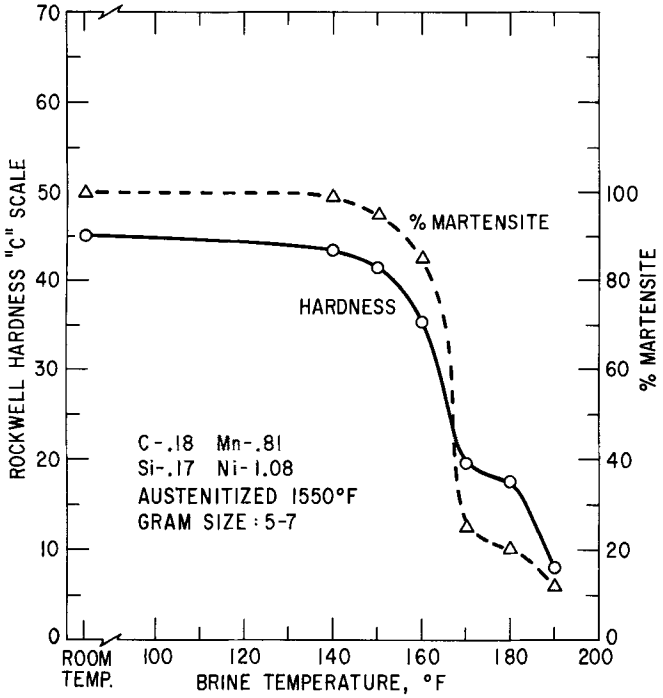

Fig. 2—Typical results of the hot-brine hardenability test.

which provides sufficient protection from scaling during the short heating period required for small specimens was therefore produced by heating within a cavity

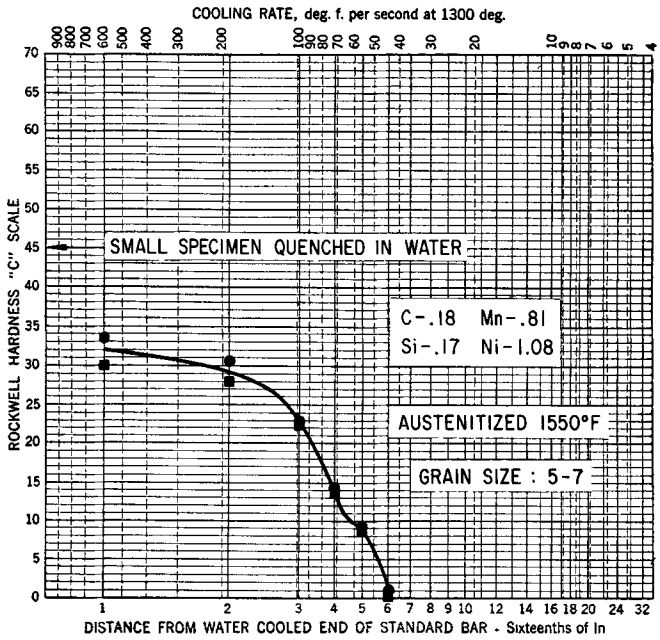

Fig. 3—End-quench hardenability test results for a low-carbon, water-hardening steel.

in a block of graphite. We bored a blind hole 1.5 in. (3.8 cm) in diam and 6 in. (15.2 cm) deep and henceforth heated in the cavity thus produced. This practice simply and effectively solved the problem of nonuniform hardness.

After testing specimens of various dimensions, we chose the one shown in Fig. 1. This specimen was made, starting with material of larger size, by hot and cold rolling to 0.1 in. (2.5 mm) thick and then shearing the 1 sq in. (25 mm) specimen from the rolled strip. The hole is used for wiring to a rod. All specimens initially were normalized from 1700°F (925°C). Each specimen was then individually austenitized and quenched in brine at a predetermined temperature. Hardness was measured, as indicated in Fig. 1, after grinding both 1 sq in. faces. The average of the five readings was taken as the hardness of the specimen. In this investigation, hardness was used mainly as a guide in selecting brine temperatures, but in routine hardenability testing, hardness can serve as an indicator of hardenability. After the hardness measurement, each specimen was cut in half and the percentage of martensite estimated visually in the central region; quantitative metallographic methods could, of course, be used but are not considered necessary for reasonably reliable and consistent results. Typical results for a representative shallow-hardening steel are shown in Fig. 2. To demonstrate the advantage of the HB test over the much-used end-quench test, Fig. 3 shows end-quench hardenability test results for the same steel. Note that at the $\frac{1}{16}$-in. (1.6 mm) location in the EQ specimen, hardness is more than 10 points lower than that of quenched martensite, and thus a critical portion of the curve is missing in Fig. 3.

THE HARDENABILITY CRITERION

To express quantitatively the hardenability effect of chemical elements or grain size, a common hardenability criterion is required. However strong the argu-

ment for the commonly used inflection point (~50 pct martensite) in the hardness-vs-distance curve of medium- and high-carbon steels, this criterion is unrealistic in the low-carbon steels of principal interest in this investigation. Instead, we chose 90 pct martensite. With more than this degree of slack quenching, mechanical properties, either before or after tempering, begin to deteriorate markedly. In a basic investigation where the highest degree of reliability is essential, it is preferable to determine the 90 pct martensite point by direct examination of microstructure rather than to rely on a less reliable but more easily determined hardness value. Therefore, from the percent martensite-vs-distance curve (Fig. 2), the brine temperature for 90 pct martensite was read off to serve as the basic hardenability criterion. This criterion proved to be a satisfactory one; it can be precisely determined, was reproducible, and distinguished between steels of only slightly different hardenability.

CORRELATION OF BRINE TEMPERATURE AT 90 PCT MARTENSITE WITH DIAMETER OF QUENCHED CYLINDERS

The brine temperature at 90 pct martensite is not, however, a satisfactory numerical hardenability index. Therefore, it is desirable to correlate it with cylinder diameters; once this is done, the direct results of HB tests can be expressed in the more meaningful terms of cylinder diameters.

Such correlation requires dual hardenability tests of a series of shallow-hardening steels covering the range in hardenability measurable by the HB test. Five steels were selected which met this requirement, and one was tested in both the fine- and coarse-grained conditions (Table I). Cylinders of various diameters were produced by swaging. The correlation is based on 90 pct martensite at the center of a cylinder or in the central area of the HB specimen; this was determined by metallographic examination. Both oil- and water-quenched cylinders were tested with results listed in Table I and plotted in Fig. 4.

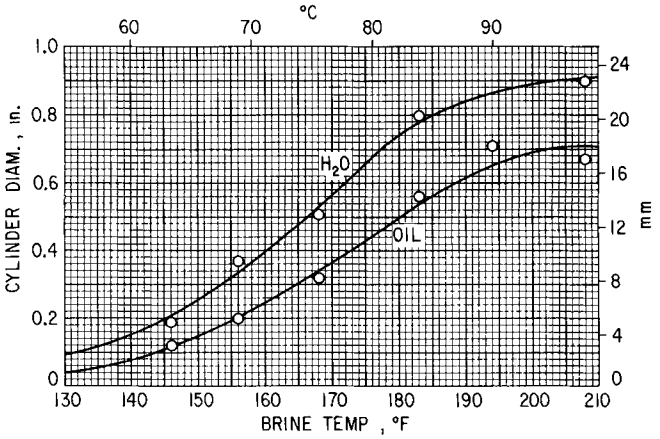

Fig. 4—Correlation of the hot-brine hardenability test with water- and oil-quenched cylinders.

The data points adequately, although not perfectly, define two curves, one for oil-quenched and the other for water-quenched cylinders. The shape of these two curves is reasonable; as brine approaches ambient temperature, the curves level off and do so again as the boiling point of brine is approached. The HB test obviously is applicable to steels which are hardenable when water-quenched in the form of cylinders 0.1 to 0.9 in. (2 to 24 mm) in diam; these, of course, are so-called shallow-hardening steels. Henceforth, the hardenability criterion used to express quantitatively HB test results will be the diameter of a water-quenched cylinder which contains 90 pct martensite at its center. The correlation chart makes it unnecessary to undertake the tedious preparation and treatment of numerous

Table I. Material, Heat Treatment, and Results of the Correlation of Hot Brine Temperature with Diameter of Quenched Cylinders

	Composition, wt pct								
Steel	C	Mn	P	S	Si	Ni	Cr	Mo	B
1021	0.20	0.81	0.003	0.008	0.16	–	–	–	
1021 + 1Ni	0.18	0.67	0.003	0.008	0.17	1.07	–	–	–
10B21 + 1Ni	0.19	0.75	0.004	0.010	0.18	1.04	–	–	0.0021
10B21 + 1Ni + Si	0.18	0.75	0.002	0.009	0.71	1.07	–	–	–
1038	0.40	0.78	0.009	0.022	0.023	0.01	0.07	0.01	–

	Heat Treatment and Results				
				Cylinder Diameter (90 pct Martensite Center), in.	
Steel	Austenitized, F	ASTM Grain Size	HB Temp, F	Oil Quench	Water Quench
1021	1600	8	146	0.12	0.19
1021 + 1Ni	1550	8	156	0.20	0.37
10B21 + 1Ni	1600	8	194	0.71	- *
10B21 + 1Ni + Si	1550	8	208	0.67	0.90
1038	1600	8	168	0.32	0.51
1038	2000	3.5	183	0.56	0.80

*Not determined because material unavailable in sufficiently large diameters.

Table II. Effect of Grain Size on Hardenability

	Austenitized		Austenitic Grain Size			Equivalent Dia of Cylinder (90 pct Martensite at Center), Fig 4
Steel	Temp, F	Time, min	ASTM No.	$d^{-1/2}$, $mm^{-1/2}$	HB Temp, F	Water Quench, in.
1021	2000	10	3.5	3	167	0.51
0.20C	1600	10	5.5	4.3	163	0.44
0.81Mn	1600	0.5	7	5.5	160	0.39
	1550	0.3	10	9.4	110	0.10
1038	2000	10	3.5	3	183	0.78
0.40C	1600	10	8	6.6	168	0.51
0.78Mn	1550	0.5 (4 cycles)	11	11.2	124	0.09
4118	2100	5	5	4	210	0.91
0.18C-0.51Cr	2000	5	5.5	4.3	200	0.89
0.79Mn-0.12Mo	1600	10	11	11.2	171	0.58
	1600	0.5	12.5	14.6	155	0.32
A36	2000	5	3.5	3	185	0.80
0.21C	1800	10	4.5	3.6	184	0.78
1.08Mn	1600	10	5.5	4.3	181	0.75
	1600	1	7.5	6	173	0.62
1021 Si-Ni	2200	5	5	4	186	0.81
0.18C-0.71Si	2000	5	6.5	5.1	178	0.71
0.75Mn-1.07Ni	1600	10	9	7.9	165	0.48
FeC Alloy	2000	5	2.5	2.5	176	0.68
0.97C	1700	10	6	4.7	165	0.48
	1535	0.5	11	11.2	122	0.09

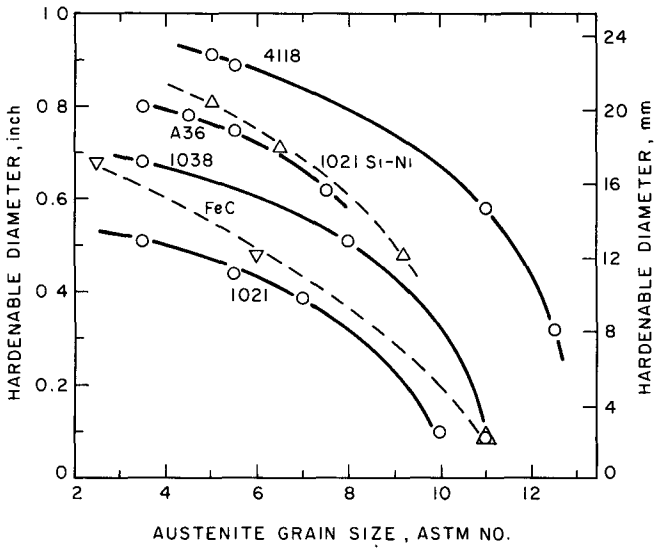

Fig. 5—Effect of grain size expressed as the ASTM number on the hardenability of six shallow-hardening steels.

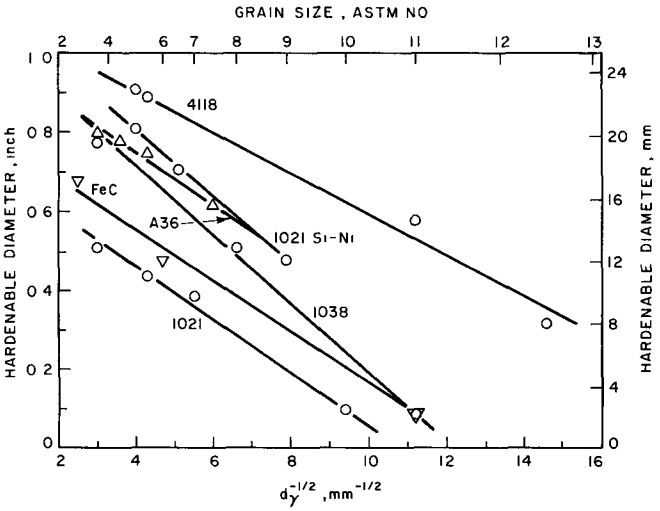

Fig. 6—Effect of grain size expressed as $d_\gamma^{-1/2}$ on the hardenability of six shallow-hardening steels.

cylinders; equivalent data can be obtained by the more convenient HB test and hardenability expressed as a meaningful parameter which can be applied to the hardening of various components using published correlation charts which relate cylinders to other shapes.

EFFECT OF VARIATION IN AUSTENITE GRAIN SIZE ON HARDENABILITY

In each of six steels, austenite grain size was varied by varying the austenitizing treatment (Table II). The six steels have different chemical compositions and hence different hardenabilities, but all are shallow-hardening steels in which hardenability is limited by transformation of austenite to grain-boundary nucleated ferrite and/or pearlite.

In Fig. 5, the data are plotted on an abscissa scale of ASTM grain-size numbers. Lines drawn through data points curve downward at small grain sizes—a trend which is very evident in those steels in which ultrafine austenite grains were developed. This trend suggests that a grain-size scale more directly related to grain-boundary area, such as the reciprocal of the square root of the mean austenite grain diameter ($d_\gamma^{-1/2}$), might convert these curves to straight lines. In Fig. 6, the data are plotted on a basic scale of $d_\gamma^{-1/2}$, with the ASTM grain size shown as an auxiliary scale at the top; on this chart, there is no difficulty in drawing a straight line through the data points for each steel. Some scatter is present, but this is to be expected due to the difficulty of precisely measuring the hardenability of shallow-hardening steels; furthermore, our grain-size ratings were made to the nearest 0.5 ASTM grain size, and this accounts for some scatter, especially when the grains are ultrafine. We did not attempt here or later in this investigation to rate austenite grain size more precisely because there is usually some variation in grain size among specimens austenitized alike; also, grains in a single specimen are seldom as uniform in size as required for more precise rating.

Fig. 7 is a generalized chart for predicting the quantitative hardenability of austenite grain size in shallow-hardening steels. In constructing this chart, a series of guidelines having the average slope of those in Fig. 6 are drawn on a chart with the water-quenched cylinder diameter with 90 pct martensite at the center as the ordinate scale and ASTM grain size as a nonuniform abscissa scale, the basic scale being $d_\gamma^{-1/2}$. This chart is used for predicting the hardenability at any desired grain size in all shallow-hardening steels, in which hardenability is limited by grain-boundary nucleated ferrite and/or pearlite. It is most unlikely that the chart can be used reliably for prediction of the grain-size effect in steels whose hardenability is limited, wholly or in part, by transformation to bainite, since this constituent is not grain-boundary nucleated and hence is less affected by grain-boundary area.

Fig. 7 is used henceforth to correct a measured hardenable diameter of steel for difference in austenite grain size between it and others in a series; the chart is also used later for estimating hardenability. For example, assume one has a result, either measured or estimated from chemical composition, which gives a hardenable diameter of 0.65 in. (16.5 mm) at 8 ASTM grain size. This point is first located on the chart, as in Fig. 7. To correct the diameter to any other grain size, a line is drawn through the point parallel to the slanting lines on the chart (the dashed line in Fig. 7) and the corrected diameter read on the ordi-

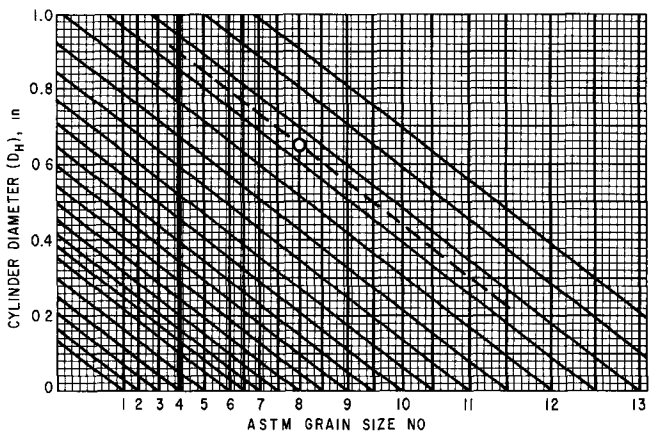

Fig. 7—Chart for predicting hardenable diameter (90 pct martensite, water quenched) for any grain size different from that at which hardenability was measured or estimated.

nate scale. Of course, in actual use a straight edge can be used, making it unnecessary to actually plot the point or to draw a line.

HARDENABILITY EFFECT OF CARBON

The quantitative hardenability effect of carbon is basic and hence should logically be evaluated before considering other elements. Therefore, seven Fe-C alloys were made by vacuum melting "Plast-iron A104" and adding graphite. The alloys were cast into 3-in.-diam (7.5 cm) 17-lb. (7.7 kg) ingots. The middle portion of each ingot was hot-rolled to 0.125-in.-thick (3.2 mm) strip and then cold-rolled to 0.1 in. (2.5 mm) thick. After normalizing from 1700°F (925°C), HB test specimens were sheared from the strip. The carbon content of the seven alloys ranged from ~0.1 to 1.0 pct; by chance, two alloys contained 0.50 pct C (Table III). Since the melting stock was 99.9 pct Fe and the only addition was graphite, the result is a series of relatively pure Fe-C alloys in which the combined effect of impurities on hardenability is small and essentially the same in all the alloys.

Table III lists the hardenability test results, directly measured as the brine temperature at 90 pct martensite. This temperature was converted, by means of Fig. 4, to the hardenable diameter which has 90 pct martensite at the center when water-quenched. Because grain size varied somewhat, when necessary the hardenable diameter was corrected by means of Fig. 7 to a common grain size of 4 ASTM.*

*The melting procedure (except for addition of alloys), preparation of HB specimens, hardenability testing, and correction for grain size for the Fe-C alloys is essentially the same as used in later "pure" Fe-C + alloy series and hence need not be repeated. In some series, additional corrections for C based on Fig. 8 and for Mn based on Fig. 12 were made.

Corrected hardenable diameters (last column, Table III) are plotted in Fig. 8 and a smooth curve drawn through the data. The two points at 0.5 pct C lie close together, which confirms the ability of the procedure to measure reproducibly the hardenability of these difficult, very-low-hardenability alloys. The curve rises steeply (C has a large hardenability effect at low concentrations), peaks at ~0.8 pct C (the eutectoid composition has maximum hardenability), and then falls off somewhat in the hypereutectoid range. This curve is a necessary basis for estimating hardenability, since all steels are Fe-C alloys with other elements present intentionally or as impurities.

HARDENABILITY EFFECT OF MANGANESE

The quantitative hardenability effect of Mn was measured in two alloy series. The first series of six alloys (Table IV) contains 0.5 pct Mn with C varying from 0.07 to 1.34 pct. In this series, austenitizing temperature was varied in an effort to develop 4 ASTM grain size in all alloys. This was successful except for the 0.78 pct C alloy whose grain size was 5 ASTM at 1600°F (870°C); this alloy could not be heated higher without developing an undesirable mixed grain size. Hardenability test results, listed in Table IV, are plotted in Fig. 9. The curve matched to data points has a similar shape to that of the Fe-C alloys (transposed from Fig. 8 and shown in Fig. 9 as a dashed-line curve), but is displaced upward due to the hardenability effect of 0.5 pct Mn.

A multiplying factor for 0.5 Mn at any carbon content can be calculated by dividing the hardenable diameter of the Fe-0.5 Mn-C alloy by that of the Fe-C alloy of corresponding carbon content. These factors, Fig. 10, decrease markedly as C increases to 0.6 pct and then level off; this result is ambiguous because it implies

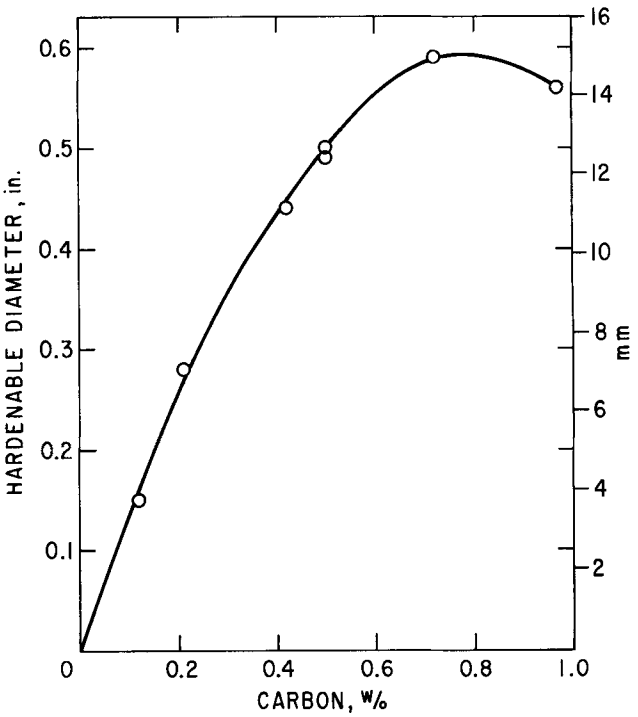

Fig. 8—Hardenability of Fe-C alloys (90 pct martensite, water quenched, no. 4 ASTM grain size).

Table III. Hardenability Test Results for Fe-C Alloys

Alloy, wt pct C	Austenitized, F	ASTM Grain Size	Brine Temp for 90 pct Martensite, F	Hardenable Diameter (90 pct Martensite, Water Quench), in.	
				Measured	Corrected
0.12	1650	4	140	0.15	0.15
0.21	1650	4	152	0.28	0.28
0.42	1650	5	160	0.39	0.44
0.50(a)	1650	4	166	0.49	0.49
0.50(b)	1650	2	171	0.58	0.50
0.72	1650	3.5	173.5	0.63	0.59
0.97	1650	5	167	0.51	0.56

Table IV. Hardenability Test Results—Fe-0.5 Mn-C Series

Alloy	Austenitized, F	ASTM Grain Size	Brine Temp for 90 pct Martensite, F	Hardenable Diameter (90 pct Martensite, Water Quench), in.	
				Measured	Corrected to 4 Grain Size
0.073C-0.49Mn	1900	4	158	0.30	0.30
0.21C-0.55Mn	1675	4	170	0.56	0.56
0.43C-0.55Mn	1675	4	176	0.68	0.68
0.58C-0.53Mn	1675	4	177	0.70	0.70
0.78C-0.49Mn	1600	5	180.5	0.75	0.80
1.35C-0.53Mn	1800	4	170	0.56	0.62

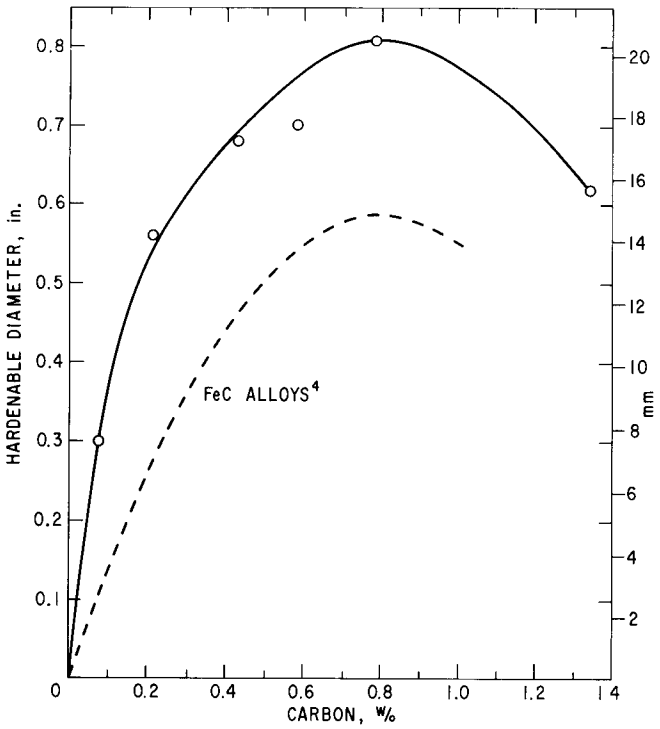

Fig. 9—Hardenability of Fe-0.5 pct Mn-C alloys compared to that of Fe-C alloys (90 pct martensite, water quenched, no. 4 ASTM grain size).

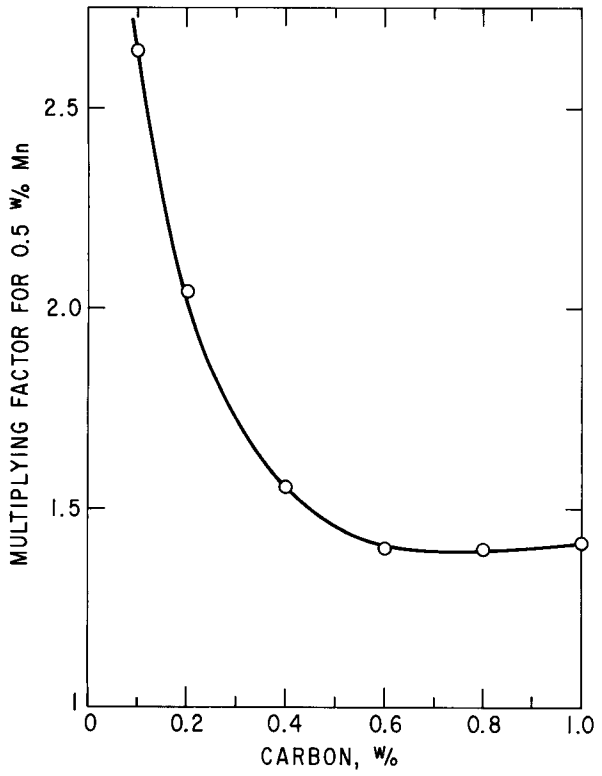

Fig. 10—Hardenability multiplying factor for 0.5 pct Mn at different carbon contents.

that the hardenability effect of Mn is much greater in low-carbon steel. Apparently, the multiplying-factor concept is unreliable for these very shallow-hardening Fe-C alloys with hardenable diameters in fractional inches. Multiplying factors were developed principally for medium-carbon, oil-hardening steels in which they have been shown[3] to be very useful in estimating hardenability from chemical composition; however, when applied to very deep-hardening steels, estimated hardenability is often too high. The multiplying-factor concept implies that the same quantitative hardenability effect is conveyed when, for example, a certain percentage of an alloying element increases the hardenable diameter from 0.25 to 0.5 in. (0.63 to 1.27 cm) as when it increases hardenable diameter from 1 to 2 in. (2.5 to 5 cm); this is contrary to the principles of heat flow. It is more realistic, over a wide range of hardenable diameters, to consider the element increasing the hardenable diameter by adding a layer of constant thickness; that is, by increasing the hardenable diameter of the base compositions by the same amount. There may be some difficulty with this approach due to very high surface/volume ratios in very small diameters, but these will often be too small to be of interest.

If, instead of adopting a multiplying factor to express the quantitative hardenability effect, we adopt instead the increase in diameter, ΔD, the effect of 0.5 pct Mn in our Fe-0.5 Mn-C alloys is constant over the entire carbon range within reasonable limits of experimental error (Fig. 11). Therefore, we will henceforth use ΔD as a means of expressing numerically the quantitative hardenability effect of any given percentage of any given element added to steel; ΔD, as used herein and explained earlier, is the increase in the diameter of

Table V. Hardenability Test Results—Mn Series

Alloy	Austenitized, F	ASTM Grain Size	Brine Temp for 90 pct Martensite, F	Hardenable Diameter (90 pct Martensite, Water Quench), in.	
				Measured	Corrected to 4 Grain Size
0.35Mn	1675 (10 min)	3.5	165	0.48	0.46
0.63Mn	1675 (10 min)	3.5	171	0.58	0.56
0.91Mn	1675 (10 min)	2.5	179	0.72	0.66
1.24Mn	1675 (10 min)	3.5	181	0.75	0.73
1.66Mn	1675 (10 min)	3.5	190	0.84	0.82
1.93Mn	1675 (10 min)	4	196	0.88	0.88
1.93Mn	1600 (20 sec)	7.5	178	0.71	0.89

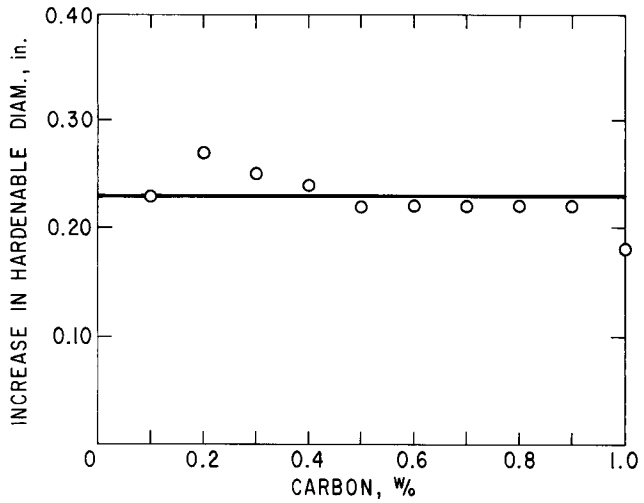

Fig. 11—Effect of 0.5 pct Mn on hardenable diameter (90 pct martensite, water quenched) at various carbon contents.

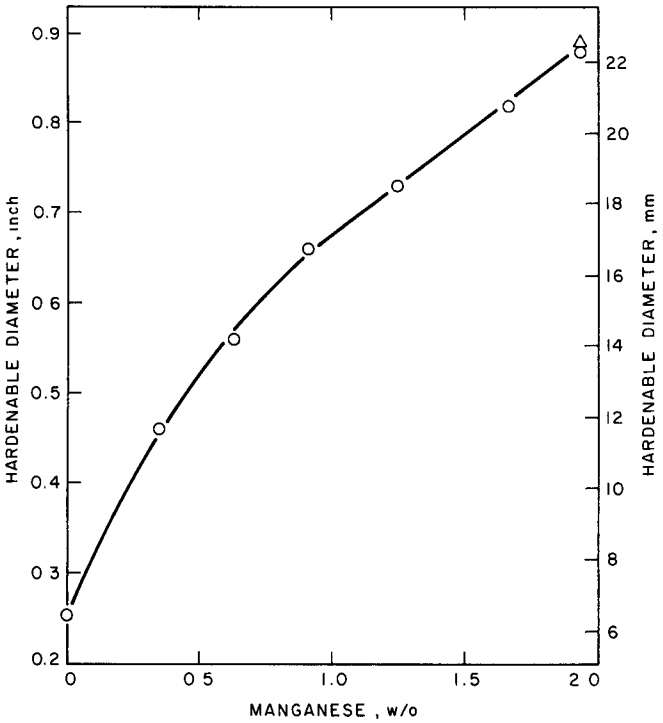

Fig. 12—Effect of Mn on hardenable diameter of 0.2 pct C-Fe-Mn alloys (90 pct martensite, water quenched, no. 4 ASTM grain size).

cylinders which when water-quenched contain 90 pct martensite at the center.

The second series of Fe-C-Mn alloys contains 0.2 pct C and Mn in the range 0.35 to 1.93 pct (Table V). There are six alloys in this series. The highest Mn (1.93 pct) was austenitized in two different ways to develop both a coarse- and a fine-grained condition (Table V); this was done both as a check on the grain-size correction (Fig. 7) and to determine whether Mn has the same hardenability effect in steel with widely different austenite grain size. The two points at 1.93 pct Mn (Fig. 12) indicate essentially the same hardenable diameter, and this confirms that the grain-size correction is reliable and that Mn has the same quantitative hardenability effect at all grain sizes.

The data points for all six Fe-Mn-0.2 C alloys lie on a smooth curve (Fig. 12). The point for 0 Mn was taken from the earlier Fe-C alloy data, and the curve extrapolates nicely to this point. Mn increases hardenability substantially and does so progressively up to 2 pct and probably well beyond. The hardenability of carbon steels is determined primarily by the combined effect of C and Mn, and the data obtained thus far provide the basic data needed for estimating the hardenability of carbon steels.

HARDENABILITY EFFECT OF OTHER ELEMENTS

A number of chemical elements are present in commercial carbon steels either as an impurity or intentionally added to enhance hardenability. It is therefore essential in estimating the hardenability of carbon steels to know the quantitative hardenability effect of additional elements. Although in respect to carbon steels, interest is limited to small percentages of residual and impurity elements, we will make measurements over most of the range of hardenability possible with the HB test, since this provides useful data for future investigation of hardenability. Graded percentages of each individual element were added to a "pure" base composition containing ~0.2 pct C and either 0.3 to 0.5 pct Mn.

Table VI. Hardenability Effect of Silicon

Alloy	Composition, wt pct C	Mn	Si
0.09Si	0.19	0.53	0.09
0.30Si	0.18	0.53	0.30
0.57Si	0.19	0.53	0.57
0.86Si	0.19	0.53	0.86

Alloy	Austenitized, F	ASTM Grain Size	Brine Temp for 90 pct Martensite, F	Hardenable Diameter (90 pct Martensite, Water Quench), in. Measured	Corrected to 4 Grain Size
0.00Si	(From Fig. 9)	–	–	–	0.51
0.09Si	1800	2.5	171	0.58	0.52
0.30Si	1800	3	175	0.66	0.62
0.57Si	1800	4	175	0.66	0.66
0.86Si	1850	4.5	175	0.66	0.68

Table VII. Hardenability Effect of Phosphorous

Alloy	Composition, wt pct C	Mn	P
0.002P	0.2*	0.5*	0.002
0.064P	0.2*	0.5*	0.064
0.28P	0.2*	0.5*	0.28

Alloy	Austenitized, F	ASTM Grain Size	Brine Temp for 90 pct Martensite, F	Hardenable Diameter (90 pct Martensite, Water Quench), in. Measured	Corrected to 4 Grain Size
0.002P	2000	4	166	0.50	0.50
0.064P	2000	3.5	175	0.66	0.64
0.28P	2000	3.5	178	0.71	0.69

*Melt aim for single heat split into 3 ingots

Silicon

The hardenability effect of Si was determined using four alloys containing 0.09, 0.30, 0.57, and 0.86 pct Si. Pertinent data for the testing of these alloys are listed in Table VI. It was necessary to adopt a relatively high austenitizing temperature to develop all austenite in the highest Si alloy. Fig. 13 is a plot of the data which indicates that Si has less hardenability effect per constant incremental addition as its concentration increases.

Phosphorus

Three alloys comprise the phosphorus series which was a single heat split into three portions with phosphorus added to the last two. Details are given in Table VII and results summarized graphically in Fig. 14.

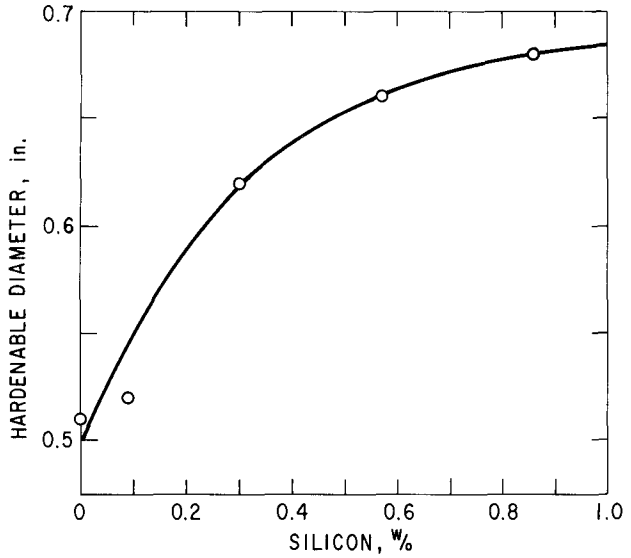

Fig. 13—Effect of Si in 0.2 pct C-0.5 pct Mn-Fe alloy on hardenable diameter (90 pct martensite, water quenched, no. 4 ASTM grain size).

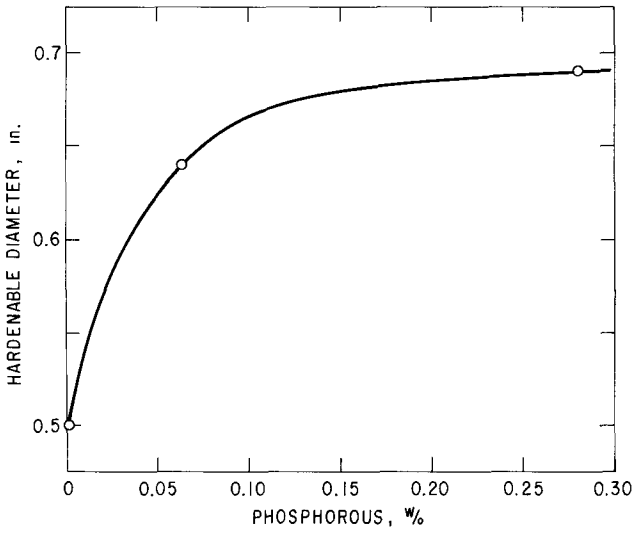

Fig. 14—Effect of P in 0.2 pct C-0.5 pct Mn-Fe alloy on hardenable diameter (90 pct martensite, water quenched, no. 4 ASTM grain size).

Table VIII. Hardenability Effect of Sulfur

Alloy	Composition, wt pct C	Mn	S
0.006S	0.19	0.55	0.006
0.03S	0.19	0.55	0.03
0.05S	0.17	0.55	0.05
0.079S	0.15	0.54	0.079

Alloy	Austenitized, F	ASTM Grain Size	Brine Temp for 90 pct Martensite, F	Hardenable Diameter (90 pct Martensite, Water Quench), in. Measured	Corrected to 0.19 pct C	Corrected to 4 Grain Size
0.006S	1775	3	170	0.56	0.56	0.52
0.03S	1650	3	170	0.56	0.56	0.52
0.5S	1800	4	165	0.48	0.52	0.48
0.079S	1850	3.5	147	0.22	0.27	0.20

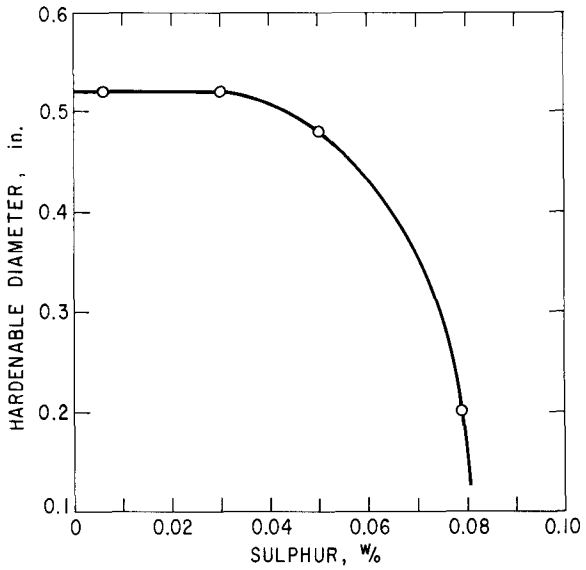

Fig. 15—Effect of S in 0.2 pct C-0.5 pct Mn-Fe alloy on hardenable diameter (90 pct martensite, water quenched, no. 4 ASTM grain size).

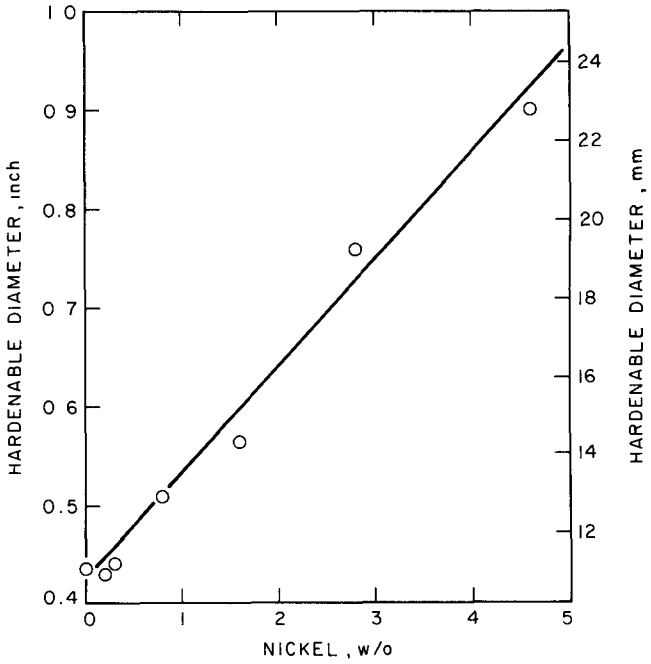

Fig. 16—Effect of Ni in 0.2 pct C-0.3 pct Mn-Fe alloy on hardenable diameter (90 pct martensite, water quenched, no. 4 ASTM grain size).

Phosphorus had a relatively potent effect in small percentages, but the curve appears to nearly level off above 0.1 pct P.

Sulfur

The four alloys used to evaluate the hardenability effect of S are listed in Table VIII. It was necessary to vary austenitizing temperature to develop in all four alloys a uniform coarse-grain size of 3 to 4 ASTM. Sulfur combines with Mn in steel to form inclusions. Therefore, S has an apparent negative effect because the loss in hardenability due to loss of Mn from solution in austenite is more than offset by any positive hardenability effect of the small concentration of S dis-

Table IX. Hardenability Effect of Nickel

Alloy	Composition, wt pct C	Mn	Ni
0.2Ni	0.16	0.34	0.20
0.3Ni	0.16	0.34	0.29
0 8Ni	0.18	0.31	0.80
1 6Ni	0.18	0.30	1 57
2 8Ni	0.19	0.36	2.84
4.6Ni	0 19	0 35	4 58

Alloy	Austenitized, F	ASTM Grain Size	Brine Temp for 90 pct Martensite, F	Hardenable Diameter (90 pct Martensite, Water Quench), in. Measured	Corrected to 0 18 pct C	Corrected to 0.35 pct Mn	Corrected to 4 Grain Size
0.00Ni	(Estimated from Figs. 8 and 12)						0.435
0.2Ni	1650	4	160	0.40	0.425	0.43	0.43
0.3Ni	1650	4	161	0.41	0.435	0.44	0.44
0.8Ni	1650	4	166	0.49	0.49	0.51	0.51
1.6Ni	1650	4	168.5	0 54	0.54	0.565	0.565
2.8Ni	1650	3.5	184	0.79	0.78	0.775	0.76
4.6Ni	1650	4	207	0.91	0 90	0.90	0.90

Table X. Hardenability Effect of Chromium

Alloy	Composition, wt pct C	Mn	Cr
0.1Cr	0 18	0.31	0.10
0.2Cr	0.18	0 32	0 18
0.4Cr	0.18	0.31	0.39
0.6Cr	0.19	0 30	0.63

Alloy	Austenitized, F	ASTM Grain Size	Brine Temp for 90 pct Martensite, F	Hardenable Diameter (90 pct Martensite, Water Quench), in. Measured	Corrected to 0.18 pct C	Corrected to 0.31 pct Mn	Corrected to 4 Grain Size
0.00Cr	(Estimated from Figs 8 and 12)						0.415
0.1Cr	1650	3	166 5	0.50	0.50	0.50	0.45
0.2Cr	1650	3	168	0.53	0 53	0.525	0.47
0.4Cr	1650	3	175	0 66	0.655	0 655	0 60
0.6Cr	1650	3	182.5	0.77	0 765	0.77	0.72

solved in austenite might have. The apparent net negative hardenability effect of S has been observed by Grossmann.[3] The quantitative hardenability effect of S is no doubt dependent, to some extent, on the amount of Mn in steel, which makes it difficult to estimate the effect of S over a wide range in steel composition. Fortunately, our data (Fig. 15) indicate that S in amounts < 0.05 pct has little or no hardenability effect. Hence, S can be ignored in estimating the hardenability of nonresulfurized steels.

Nickel

Table IX lists the alloys used and the results of the investigation of the effect of Ni in 0.2 C-0.3 Mn-Fe alloys. In this series, as well as in several others to follow, Mn in the base composition was reduced to increase the amount of alloy which could be added without exceeding the maximum hardenable diameter measurable with the HB test. The data (Fig. 16) indicate that Ni has only a small hardenability effect in amounts likely to be present as a residual element in carbon steels.

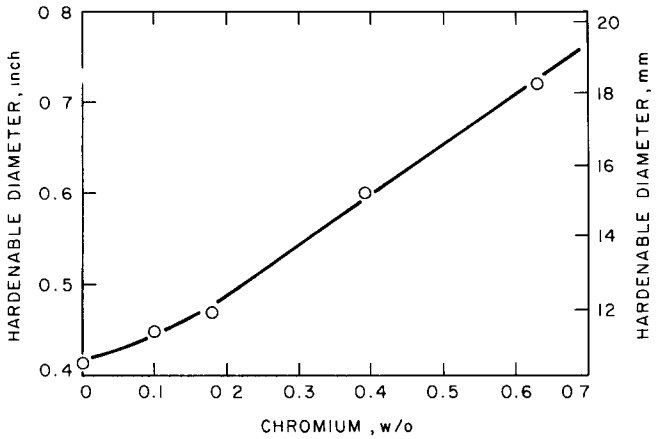

Fig. 17—Effect of Cr in 0.2 pct C-0.3 pct Mn-Fe alloy on hardenable diameter (90 pct martensite, water quenched, no. 4 ASTM grain size).

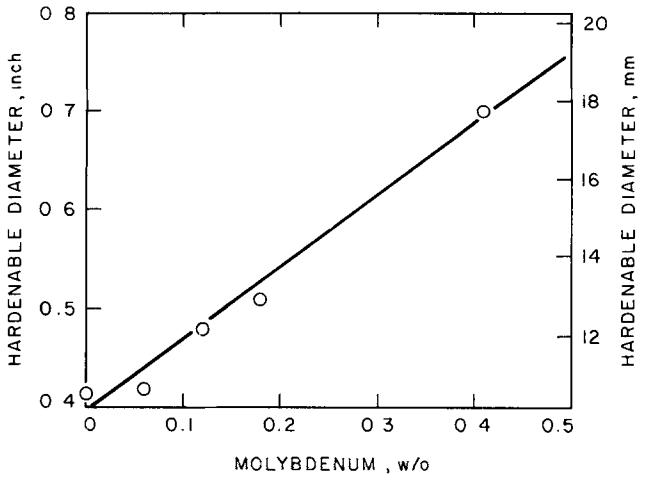

Fig. 18—Effect of Mo in 0.2 pct C-0.3 pct Mn-Fe alloy on hardenable diameter (90 pct martensite, water quenched, no. 4 ASTM grain size).

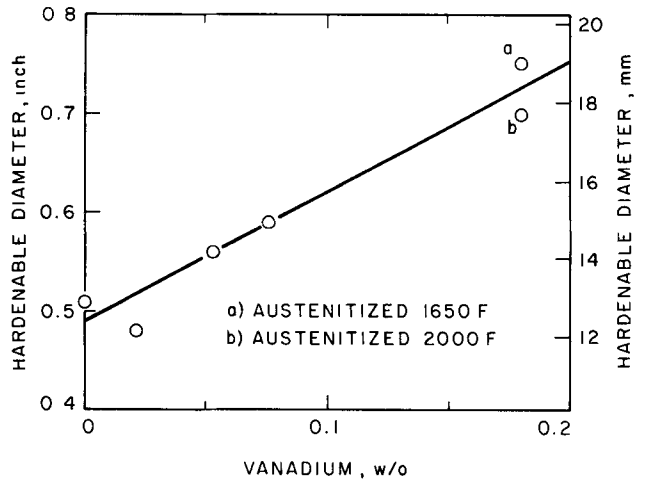

Fig. 19—Effect of V in 0.2 pct C-0.5 pct Mn-Fe alloy on hardenable diameter (90 pct martensite, water quenched, no. 4 ASTM grain size).

Chromium

The quantitative hardenability effect of Cr was evaluated in the four alloys listed in Table X. Fig. 17 is a plot of the data indicating that Cr in amounts well under 1 pct substantially increases hardenability.

Molybdenum

In the four alloys containing Mo (Table XI), it was necessary to vary the austenitizing to avoid mixed grain size but by so doing all developed the desired 4 ASTM grain size. The data points seem to lie on a straight line (Fig. 18) with Mo having a relatively large hardenability effect in small concentrations.

Vanadium

The four alloys containing V were not matched in grain size when austenitized at 1650°F (900°C) because in the highest V alloy, the grain size remained uniformly fine (Table XII). Therefore, the 0.2 V alloy was also austenitized at 2000°F (1095°C) to develop uniform large grains; additionally, raising the austenitizing temperature would tend to dissolve more V, if any were undissolved at 1650°F (900°C). In Fig. 19, there are accordingly two points at 0.18 pct V. After correcting to a common grain size of 4 ASTM, they lie reasonably close together, one above and one below the line as drawn; this result indicates that a higher-than-normal austenitizing temperature is not required for essentially full solution of 0.18 pct V in an 0.2 pct C steel. A substantial increase in hardenability is indicated for relatively small percentages of V.

Titanium

We anticipated some difficulty in evaluating the hardenability effect of Ti. Titanium combines strongly with C and N in steel and forms particles which dissolve gradually as the austenitizing temperature is higher. Because C and N in solution increase hardenability, Ti could, under some circumstances, conceivably have an apparent net negative hardenability effect, even though Ti itself no doubt increases hardenability. Thus, the quantitative hardenability effect of Ti is likely to vary with C and N in steel and also with austenitizing temperature.

Table XI. Hardenability Effect of Molybdenum

Alloy	Composition, wt pct C	Mn	Mo
0.6Mo	0.18	0.31	0.06
0.12Mo	0.18	0.31	0.12
0.18Mo	0.18	0.31	0.18
0.41Mo	0.18	0.31	0.41

Alloy	Austenitized, F	ASTM Grain Size	Brine Temp for 90 pct Martensite, F	Hardenable Diameter (90 pct Martensite, Water Quench), in Measured
0.00Mo	(Estimated from Figs 8 and 12)			0.415
0.06Mo	1650	4	161.5	0.42
0.12Mo	1800	4	165	0.48
0.18Mo	1800	4	167	0.51
0.41Mo	1900	4	177.5	0.70

Table XII. Hardenability Effect of Vanadium

Alloy	Composition, wt pct C	Mn	V
0.02V	0.19	0.52	0.021
0.05V	0.19	0.52	0.052
0.1V	0.19	0.51	0.076
0.2V	0.19	0.51	0.18

Alloy	Austenitized, F	ASTM Grain Size	Brine Temp for 90 pct Martensite, F	Hardenable Diameter (90 pct Martensite, Water Quench), in. Measured	Corrected to 0.53 pct Mn	Corrected to 4 Grain Size
0.00V	(Estimated from Figs. 8 and 12)					0.51
0.02V	1650	3.5	166	0.50	0.50	0.48
0.05V	1650	3.5	171	0.58	0.58	0.56
0.1V	1650	3.5	172.5	0.61	0.615	0.59
0.2V	1650	7	171.5	0.59	0.595	0.75
0.2V	2000	3	180	0.74	0.745	0.70

Table XIII. Hardenability Effect of Titanium

Alloy	Composition, wt pct C	Mn	Ti
0.02Ti	0.20	0.51	0.026
0.05Ti	0.19	0.51	0.062
0.1Ti	0 20	0.52	0.12
0.2Ti	0.20	0.52	0.21

Alloy	Austenitized, F	ASTM Grain Size	Brine Temp for 90 pct Martensite, F	Hardenable Diameter (90 pct Martensite, Water Quench), in. Measured	Corrected to 0.20 pct C	Corrected to 0.51 pct Mn	Corrected to 4 Grain Size
0.00Ti	(Estimated from Figs. 8 and 12)						0.51
0.02Ti	1650	8	140	0.16	-	-	0.41
	2000	3.5	165.5	0 49	-	-	0.47
0.05Ti	1650	9	137	0.13	0 14	-	0.48
	2000	3	170	0.56	0 57	-	0.53
0 1Ti	1650	9.5	130	0.10	-	0 095	0.50
	2000	3.5	175	0.66	-	0.655	0.63
0.2Ti	1650	9 5	130	0.10	-	0.095	0.50
	2000	3	173	0.62	-	0.615	0.57

Table XIV. Hardenability Effect of Zirconium

Alloy	Composition, wt pct C	Mn	Zr
0 02Zr	0.19	0 52	0 026
0 05Zr	0.19	0 52	0 056
0 1Zr	0 19	0.53	0 10
0 2Zr	0.19	0.53	0 20

Alloy	Austenitized, F	ASTM Grain Size	Brine Temp for 90 pct Martensite, F	Hardenable Diameter (90 pct Martensite, Water Quench), in. Measured	Corrected to 0 52 pct Mn	Corrected to 4 Grain Size
0.00Zr	(Estimated from Figs. 8 and 12)					0.51
0.02Zr	1650	3.5	165	0.48	-	0.46
0.05Zr	1650	3.5	161	0.415		0 40
0.1Zr	1900	3.5	160	0.40	0.395	0 38
0.2Zr	1900	4	140	0.15	0 145	0.145

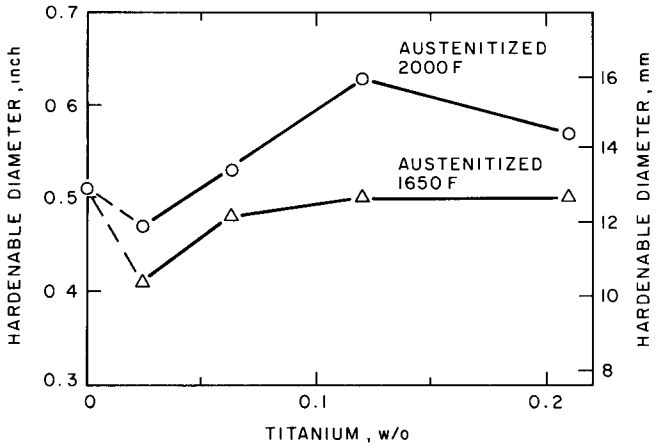

Fig. 20—Effect of Ti in 0.2 pct C-0.5 pct Mn-Fe alloy on hardenable diameter (90 pct martensite, water quenched, no. 4 ASTM grain size).

The four alloys containing graded percentages of Ti (Table XIII) were tested both as austenitized at 1650°F (900°C) and as austenitized at 2000°F (1095°C); the former were uniformly fine-grained and the latter uniformly coarse-grained. In addition to the difference in grain size, more Ti was probably dissolved in austenite at the higher temperature. The results of our tests (Table XIII and Fig. 20) indicated, as expected, a greater hardenability effect of Ti at the higher temperature. There seems to be a decrease in hardenability with the smallest Ti addition (0.026 pct) at both austenitizing temperatures. The data indicate complex behavior for Ti rather than the consistent and progressive hardenability increase observed in most other alloying elements. Faced with this situation, it seems unwise to try to estimate the quantitative hardenability effect of the small amount of Ti present in commercial carbon steels; fortunately, it is likely to be sufficiently small to be neglected without serious error.

Zirconium

In the Zr series (Table XIV), some difficulty was encountered in developing a uniform coarse-grain size because the two highest Zr alloys had a higher coarsening temperature than the two lowest. However, by austenitizing the former at 1900°F (1040°C) and the latter at 1650°F (900°C), a reasonably good match in grain size was obtained. The results (Table XIV and Fig. 21) reveal a definite negative hardenability effect in these alloys. Zr resembles Ti in forming difficult-to-dissolve carbides and nitrides, and the observed negative hardenability effect of Zr may be explained by failure to dissolve much Zr in austenite, with the undissolved Zr tying up some C and N. The presence of more undissolved particles in our specimens as Zr was higher tends to confirm this hypothesis. A negative effect of Zr such as revealed by our data has not, however, been found by others.[4,5] Consequently, the present data should be verified by additional investigation. Possibly, Zr is an element which, like Ti, varies in its hardenability effect depending on C and N in steel and on the manner in which it is austenitized. In any event, the quantitative hardenability effect of the small

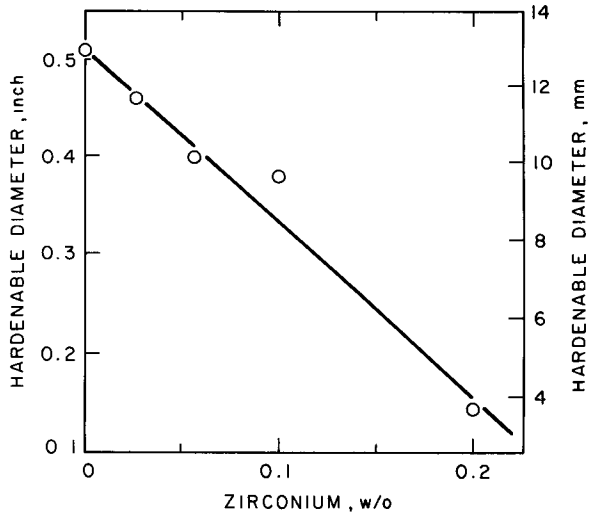

Fig. 21—Effect of Zr in 0.2 pct C-0.5 pct Mn-Fe alloy on hardenable diameter (90 pct martensite, water quenched, no. 4 ASTM grain size).

amount of Zr usually present in commercial carbon steels is small and probably best neglected in estimating hardenability.

Copper

The hardenability effect of Cu has previously been determined by quenching cylinders of AISI 1045 steel in brine.[6] Because the hardenability effect of Cu in the small residual percentages likely in commercial carbon steels is small, the results of this earlier investigation (Fig. 22), although differing in experimental technique, are probably satisfactory for estimating the hardenability of carbon steels wherein Cu is present as an impurity.

METHOD OF ESTIMATING HARDENABILITY

All data required for estimation of the hardenability of carbon steels from chemical composition and grain size have been obtained. The method of estimation proposed is simple and direct. A numerical hardenability criterion is required, and it will be the diameter (D_H) in in.* of the cylinder** which contains 90 pct martensite at the center when water-quenched.

*In accordance with past hardenability evaluation, the inch scale, rather than the metric scale, is adopted for calculation and expressing the result; inches are easily converted to the metric system by the relationship, 1 in = 2.54 cm.

**As used here, cylinder implies a round specimen whose length is equal to or greater than 3X diam.

It is assumed that D_H for pure iron is essentially zero. The quantitative hardenability effect of carbon is expressed as an increase in diameter, ΔD_C. Alloying and impurity elements are handled similarly by individual ΔD values. The experimental data presented earlier are replotted in chart form with suitable coordinate lines to facilitate reading ΔD values as a function of weight percentage of each element (Figs. 23 and 24). Two charts, rather than one, are included to avoid confusion in the curves near the zero corner and to expand the composition scale for P and V. A curve for S is omitted because this element had no significant hardenability effect in unresulfurized steel. Curves for Ti and Zr are also omitted because these elements had a variable hardenability effect depending on the C and N content of a particular steel; since neither are ordinarily present in an amount greater than 0.05 pct in commercial carbon steels, their hardenability effect is, at most very small.

The equation for estimating hardenability, therefore, is

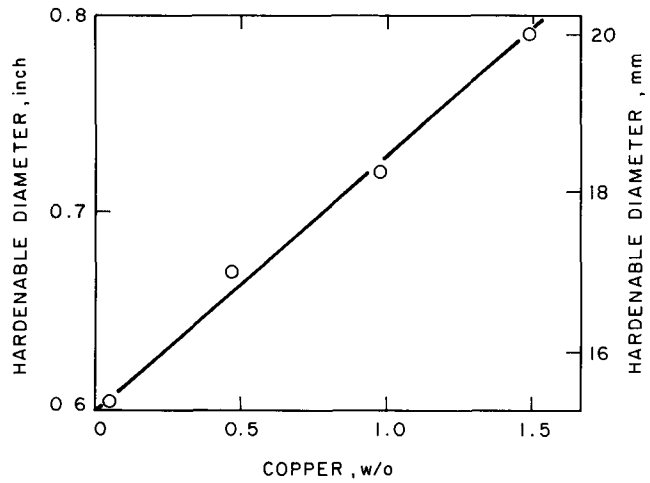

Fig. 22—Effect of Cu in AISI 1045 steel on hardenable diameter (90 pct martensite, brine-quenched).

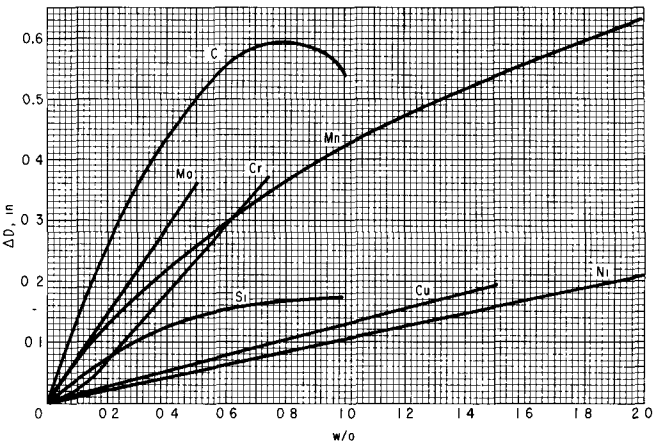

Fig. 23—Change in hardenable diameter (ΔD) with C, Mn, Si, Cu, Ni, Cr, and Mo.

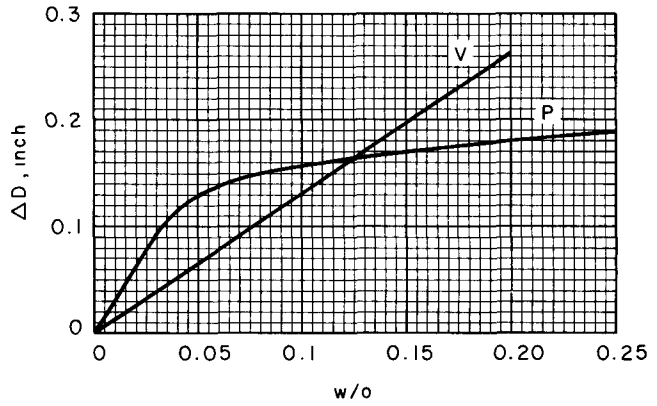

Fig. 24—Change in hardenable diameter (ΔD) with V and P.

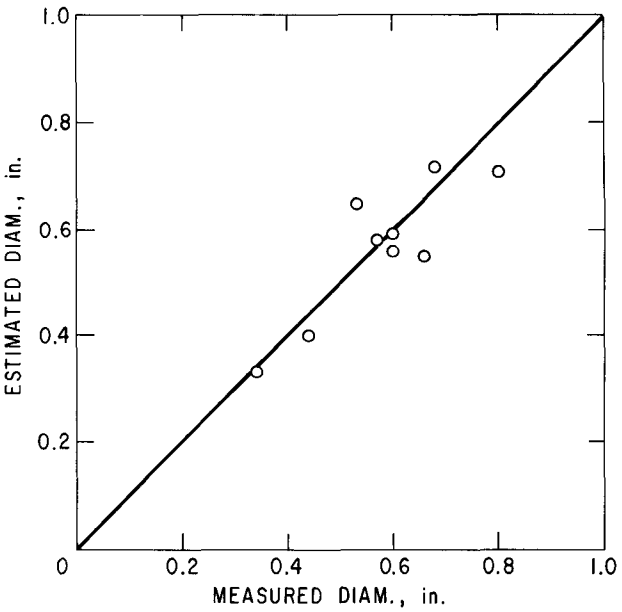

Fig. 25—Correlation of estimated and measured hardenable diameters in nine carbon steels.

$$D_H(\text{in.}) = \Delta D_C + \Delta D_{Mn} + \Delta D_P + \Delta D_{Si} + \Delta D_{Cu} + \Delta D_{Ni} + \Delta D_{Cr} + \Delta D_{Mo} + \Delta D_V$$

Where an element is present in an insignificant amount or not included in routine chemical analysis, its ΔD drops out of the equation. The remaining ΔD values read from Figs. 23 and 24 are substituted and added to give the estimated hardenable diameter.

The data, and hence the ΔD values, are for an austenite grain size of 4 ASTM. D_H, as calculated, therefore represents this grain size only and must be corrected for any other grain size by using Fig. 7.

A complete example of an estimation for a hypothetical steel containing all pertinent chemical elements is given in Table XV. Of course, few, if any, commercial carbon steels would contain all these elements in significant amounts, and estimation in the example is purposely more complicated than any likely to be encountered.

COMPARISON OF MEASURED AND ESTIMATED HARDENABLE DIAMETERS

To demonstrate the reliability of hardenability estimated as described above, the hardenabilities of the nine steels listed in Table XVI were both measured and estimated. These are all carbon steels with very low, and hence negligible, residual elements. The hardenable diameters of each steel as estimated and as measured are listed in Table XVI and shown graphically in Fig. 25. Points lie on or reasonably near the line of perfect correlation. It is unrealistic to expect perfect correlation, and the fact that points lie about equally above and below the line is evidence that the method of estimation is reasonably good.

Table XV. Example Illustrating Method of Estimating Hardenability

Chemical Composition, wt pct: C-0.24 Mn-0.78 P-0.025 S-0.022 Si-0.24 Cu-0.15 Ni-0.14 Cr-0.12 Mo-0.05 V-0.03 Ti-0.02 Zr-0.01

Grain Size 8 ASTM

Formula $D_H(\text{in.}) = \Delta D_C + \Delta D_{Mn} + \Delta D_P + \Delta D_{Si} + \Delta D_{Cu} + \Delta D_{Ni} + \Delta D_{Cr} + \Delta D_{Mo} + \Delta D_V$ (Neglect S, Ti, and Ze)

From Fig. 23: $\Delta D_C = 0.30$, $\Delta D_{Mn} = 0.355$, $\Delta D_{Si} = 0.085$, $\Delta D_{Cu} = 0.02$, $\Delta D_{Ni} = 0.015$, $\Delta D_{Cr} = 0.03$, $\Delta D_{Mo} = 0.045$

From Fig. 24 $\Delta D_P = 0.08$, $\Delta D_V = 0.04$

Summation $D_H = 0.97$ in. at 4 ASTM Grain Size

From Fig. 7 $D_H = 0.72$ in. at 8 ASTM Grain Size

Table XVI. Comparison of Estimated and Measured Hardenability

Composition, wt pct					ASTM	Hardenable Diameter in.	
C	Mn	P	S	Si	Grain Size	Estimated	Measured
0.15	0.47	0.013	0.020	0.23	8	0.33	0.34
0.16	1.23	0.013	0.020	0.26	8	0.59	0.60
0.19	0.54	0.016	0.030	0.22	8	0.40	0.44
0 19	0.59	0.017	0.036	0.18	5.5	0.58	0.57
0.21	1.08	0.008	0.024	0 028	4.5	0.72	0 78
0 22	0.84	0.015	0 021	0.26	8	0.55	0 66
0.29	1.18	0.013	0.028	0.26	8	0.71	0.80
0.31	0.47	0.011	0.021	0.24	7	0.56	0.60
0 40	0.78	0.009	0.022	0 23	8	0.65	0 53

DISCUSSION

The method in common use for estimating hardenability from chemical composition expresses the quantitative hardenability effect of a particular percentage of each alloying element as a multiplying factor.[3] This investigation suggests that, at least in shallow-hardening carbon steels, the multiplying-factor concept is less satisfactory than a system in which the quantitative hardenability effect is expressed as an increase in hardenable diameter. The new method also avoids the ideal-diameter concept which, to be applicable over a wide range in hardenable diameters, requires that severity of a particular quenchant and quenching technique be independent of size of cross section; this has been shown to be incorrect.[7]

The new method was developed for carbon steels wherein hardenability is due primarily to carbon and manganese, with residual elements playing a very minor role. Future work should investigate the possibility of extending the method to low-alloy steels. In so doing, several complications will no doubt arise. There is, for example, the probability of a different quantitative hardenability effect due to variation of austenite grain size in many low-alloy steels than herein reported for carbon steels in which the austenite transformation products which limit hardenability are strongly grain-boundary nucleated. Furthermore, a hardenability criterion based on 90 pct martensite will be regarded by many as unrealistic in bainitic-hardening steels. Current difficulty in reliably estimating the hardenability of steel is likely due, in large part, to applying the same hardenability factors over too wide a range in chemical composition, ignoring alloy-interaction effects related to a changeover from ferrite and/or pearlite to bainite as the hardenability-limiting microconstituent.

Although based on a different hardenability criterion, the relative hardenability effects of the principal alloying elements in our low-carbon, "pure" steels are similar to those reported in the literature.[2] In respect to quantitative hardenability effects, however, it is difficult to determine how our results compare with those in the literature because different investigators report rather widely different quantitative effects for each of the various alloying elements.

Hardenability is a complex property of steel and hence is probably best studied initially in carbon steels. In so doing, this investigation provides a logical base from which to proceed to additional studies of the hardenability of low-alloy steels.

SUMMARY

A new method of measuring hardenability using small specimens of fixed dimensions quenched in controlled-temperature brine was developed and correlated with the diameter of water-quenched cylinders. The hardenability criterion (D_H) adopted is 90 pct martensite at the center of a water-quenched cylinder. This method of measuring hardenability is limited to shallow-hard-

ening steels whose hardenable diameter is less than 1 in. (2.54 cm).

The quantitative hardenability effect of variation in austenite grain size was evaluated for several steels. D_H was found to vary linearly with $d_\gamma^{-1/2}$, where d is the mean austenite grain diameter. This relationship in its quantitative aspects applies only to shallow-hardening steels whose hardenability is limited by grain-boundary nucleated ferrite and/or pearlite.

The hardenability of a series of Fe-C alloys containing graded percentages of C was measured. The resulting data plot is a curve with a maximum at 0.8 pct C. D_H can be read from the curve and is the hardenability of Fe-C bases of all steels, uncomplicated by alloy or impurity effects.

The quantitative hardenability effect of 0.5 pct Mn added to "pure" Fe-C alloys was determined over a wide range of carbon and found to be the same when expressed as the increase in D_H, but not when expressed as a multiplying factor. This result led us to abandon the multiplying-factor concept heretofore used in estimating hardenability from chemical composition. The relation between D_H and percent Mn was evaluated in a series of 0.2 C-Fe alloys with graded percentages of Mn.

The individual elements, P, S, Si, Ni, Cr, Mo, V, Ti, and Zr, were added to "pure" Fe-C alloys containing 0.2 pct C and 0.3 or 0.5 pct Mn and their quantitative hardenability effect evaluated for a common grain size of 4 ASTM. With the exception of S, Ti, and Zr, these elements progressively increased hardenability as the amount added increased. The hardenability effect of Cu was based on earlier data for Cu added to an AISI 1045 steel.

A method of estimating the hardenability of carbon steels is based on the equation

$$D_H = \Delta D_C + \Delta D_{Mn} + \Delta D_P + \Delta D_{Si} + \Delta D_{Cu} + \Delta D_{Ni} + \Delta D_{Cr} + \Delta D_{Mo} + \Delta D_V$$

where the ΔD's represent the increase in hardenable diameter contributed by the percentage of each individual element present; these ΔD values are read from a chart. The result is a hardenable diameter for an austenite grain size of 4 ASTM which is corrected to any other grain size by the D_H vs $d_\gamma^{-1/2}$ relation.

In nine carbon steels, the D_H value thus estimated agreed reasonably well with the value measured, indicating that it is possible to estimate the hardenability of carbon steels from their chemical composition and austenite grain size with a useful degree of reliability.

ACKNOWLEDGMENTS

The author gratefully acknowledges the valuable assistance of C. R. Hribal in making hardenability measurements and of P. G. Fleck in preparing the many "pure" alloys used in the investigation; both are associates of the author at the United States Steel Research Laboratory.

REFERENCES

1. G T. Brown and B. A. James *Low-Alloy Steels*, p 9, The Iron and Steel Institute, London, 1968.
2. J M. Hodge *Metals Handbook*, p. 494, 1948 Edition, ASM, Metals Park, Ohio
3. M. A. Grossmann *Trans. TMS-AIME*, 1942, vol 150, p. 227.
4. W. Crafts and J. L. Lamont *Trans. TMS-AIME*, 1944, vol. 158, p. 157.
5. I. R. Kramer, S. Siegel, and J. G. Brooks *Trans. TMS-AIME*, 1946, vol 167, p 670.
6. R. A. Grange, V. E. Lambert, and J. J. Harrington *Trans. ASM*, 1959, vol. 51, p. 377.
7. D. J. Carney and A. D. Janulionis *Trans. ASM*, 1951, vol. 43, p. 480.